2011 International Symposium on Nonlinear Theory and its Applications
NOLTA2011, Kobe, Japan, September 4-7, 2011

Identification of Number of Target Image Regions Based on Bifurcation of Fixed Point in Discrete-Time Coupled Neuronal System

Ken'ichi Fujimoto†, Mio Kobayashi‡, Tetsuya Yoshinaga†, and Kazuyuki Aihara§

†Institute of Health Biosciences, The University of Tokushima
3-18-15 Kuramoto, Tokushima 770-8509, Japan
‡Department of Systems and Control Engineering, Anan National College of Technology
265 Aoki Minobayashi, Anan, Tokushima 774-0017, Japan
§Institute of Industrial Science, The University of Tokyo
4-6-1 Komaba, Meguro-ku, Tokyo 153-8505, Japan
Email: {fujimoto, yosinaga}@medsci.tokushima-u.ac.jp, kobayashi@anan-nct.ac.jp, aihara@sat.t.u-tokyo.ac.jp

Abstract—We developed a discrete-time coupled neuronal system that can extract image regions in a given image and exhibit them in a time series. We call this function "dynamic image segmentation", and it is performed by synchronizing the oscillatory responses from discrete-time neurons. In this paper, we describe how the topological property of a fixed point in the system gives significant information on the structure of regions in a given image. We also suggest a novel way to identify the number of image regions without performing a segmentation process.

1. Introduction

We developed a discrete-time coupled neuronal system for dynamic image segmentation [1]. Our system consists of a global inhibitor and neurons arranged in a grid so that a neuron corresponds to a pixel in an input image. Dynamic image segmentation is performed by the neurons' oscillatory responses, which are formed by periodic points. The type of a periodic point that appears in a steady state determines the feasibility of dynamic image segmentation. Appearance depends on parameter values, so we tuned parameter values for dynamic image segmentation based on the results of bifurcation analysis for periodic points and a fixed point in reduced models of our systems [2, 3].

In this paper, we describe how the topological property of a fixed point, which corresponds to non-oscillatory responses is unsuitable for dynamic image segmentation, gives significant information on the structure of regions in a given image. In concrete terms, by computing the characteristic multipliers of a fixed point when it bifurcates, we can identify the number of image regions and background pixels. This fact is not only informative in image segmentation but also interesting from the viewpoint of bifurcation theory.

2. Dynamic Image Segmentation System

Figure 1 shows the architecture of our neuronal system for dynamic image segmentation [1]. It consists of a global inhibitor and N neurons arranged in a grid so that one corresponds to a pixel in an N-pixel input image.

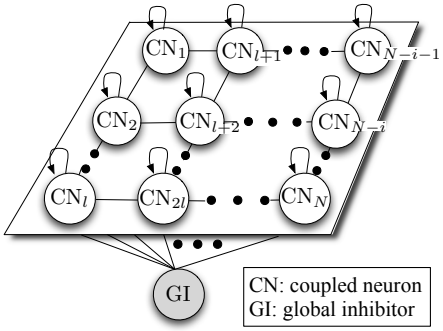

Figure 1: Architecture of proposed neuronal system.

The dynamics of the ith neuron is defined by

$$x_i(t+1) = k_f x_i(t) + d_i - W_z g(z(t), \theta_z) + \frac{W_x}{M_i} \sum_{j \in L_i} g(x_j(t) + y_j(t), \theta_c) \quad (1)$$

$$y_i(t+1) = k_r y_i(t) - \alpha g(x_i(t) + y_i(t), \theta_c) + a. \quad (2)$$

$t \in \mathbb{Z}$ denotes the discrete time where $\mathbb{Z}$ expresses the set of integers and d_i represents the direct current input with a value set by the feature value of the ith pixel in an input image. We used pixel values as feature values. The third and fourth terms on the right side of Eq. (1) correspond to suppressive input from a global inhibitor and excitatory input from neighboring neurons, including itself. W_z and W_x denote coupling strength; L_i and M_i correspond to the set of the ith neuron and its four neighboring ones and the number of elements in L_i. The dynamics of the global inhibitor is defined as

$$z(t+1) = \phi \left\{ g\left(\sum_{k=1}^{N} g(x_k(t) + y_k(t), \theta_f), \theta_d \right) - z(t) \right\} \quad (3)$$

so that it can detect one or more firing neurons and can excite itself simultaneously. $g(\cdot, \cdot)$ in Eqs. (1)–(3) represents

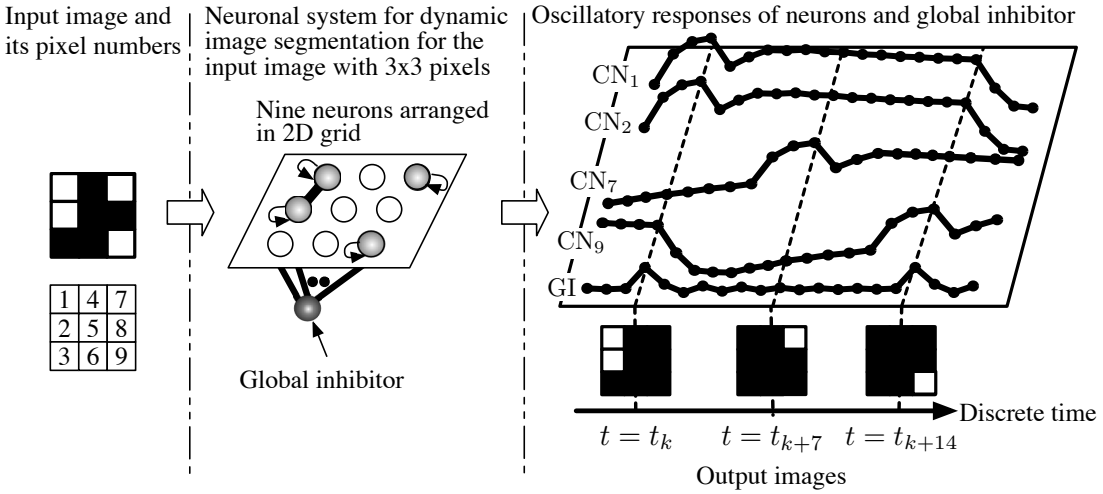

Figure 2: Scheme of dynamic image segmentation using proposed system.

the output function of a neuron or a global inhibitor and is defined by

$$g(u,\theta) = 1/\left(1+\exp(-(u-\theta)/\varepsilon)\right). \tag{4}$$

In Eqs. (1)–(4), k_f, d_i, W_z, θ_z, W_x, θ_c, k_r, α, a, ϕ, θ_f, θ_d, and ε are system parameters.

Let us illustrate the behavior of our system and the scheme of dynamic image segmentation for a binary (black and white) image (shown in Fig. 2). Despite a discrete-time dynamical system, neurons corresponding to white pixels can generate oscillatory responses formed by periodic points. Also, each neuron corresponding to a white pixel can be coupled with others corresponding to only white pixels in its neighborhood, including itself. The global inhibitor is connected to all the neurons and suppresses their activity levels when one or more neurons fire. This causes synchronized responses from directly coupled neurons and out-of-phase responses from uncoupled ones. Associating the output value of the ith neuron with the ith pixel value every discrete time enables the segmented images to be output and exhibited in a time series. This is how our system works as a dynamic image segmentation system.

3. Fixed Point and its Bifurcation

Let $\boldsymbol{x}(t) = (x_1(t), y_1(t), \ldots, x_N(t), y_N(t), z(t))^\top \in \mathbb{R}^S$, where $S = 2N+1$. $\top$ and $\mathbb{R}$ denote the transpose of a vector and the set of real numbers, respectively. The dynamics of our discrete-time dynamical system for an N-pixel image is described as

$$\boldsymbol{x}(t+1) = \boldsymbol{f}(\boldsymbol{x}(t)), \tag{5}$$

and equivalently, its iterated map defined by

$$\boldsymbol{f} : \mathbb{R}^S \to \mathbb{R}^S; \boldsymbol{x} \mapsto \boldsymbol{f}(\boldsymbol{x}), \tag{6}$$

where the nonlinear function $\boldsymbol{f} = (f_1, f_2, \ldots, f_S)^\top$ is described as

$$\boldsymbol{f} = \begin{pmatrix} k_f x_1 + d_1 - W_z g(z,\theta_z) + \dfrac{W_x}{M_1}\displaystyle\sum_{j\in L_1} g(x_j+y_j,\theta_c) \\ k_r y_1 - \alpha g(x_1+y_1,\theta_c) + a \\ \vdots \\ k_f x_N + d_n - W_z g(z,\theta_z) + \dfrac{W_x}{M_N}\displaystyle\sum_{j\in L_N} g(x_j+y_j,\theta_c) \\ k_r y_N - \alpha g(x_n+y_n,\theta_c) + a \\ \phi\left\{ g\left(\displaystyle\sum_{k=1}^{N} g(x_k+y_k,\theta_f),\theta_d\right) - z \right\} \end{pmatrix}. \tag{7}$$

Here, we define the fixed point and its characteristic multiplier. A point $\boldsymbol{x}^* \in \mathbb{R}^S$ satisfying

$$\boldsymbol{x}^* - \boldsymbol{f}(\boldsymbol{x}^*) = \boldsymbol{0} \tag{8}$$

becomes a fixed point of $\boldsymbol{f}$. The characteristic equation of $\boldsymbol{x}^*$ is defined by

$$\boldsymbol{\chi}(\boldsymbol{x}^*, \mu) = \det\left(\mu \boldsymbol{E} - D\boldsymbol{f}(\boldsymbol{x}^*)\right) = 0, \tag{9}$$

where $\boldsymbol{E}$, $D\boldsymbol{f}(\boldsymbol{x}^*)$, and $\mu \in \mathbb{C}$ correspond to the $S \times S$ identity matrix, the Jacobian matrix of $\boldsymbol{f}$ at $\boldsymbol{x} = \boldsymbol{x}^*$, and one of the S characteristic multipliers for $\boldsymbol{x}^*$; $\mathbb{C}$ denotes the set of complex numbers. Note that all the elements of $D\boldsymbol{f}(\boldsymbol{x}^*)$ can be analytically computed.

The topological property of a fixed point is determined on the basis of the arrangement of all characteristic multipliers. When one or more characteristic multiplier of a fixed point is on the circumference of a unit circle in the complex plane, the topological property of the fixed point

is changed, and then its bifurcation occurs. For example, Neimark-Sacker bifurcation occurs if one or more pairs of complex-conjugate characteristic multipliers are on the circumference. The bifurcation types and a method to compute a bifurcation point are described in Ref. [4].

Next, we introduce the previously analyzed results [2, 3] for bifurcations of a fixed point observed in reduced models of our system. The reduced models are based on the fact that plural neurons in an image region can be reduced to a neuron if we assume that the responses of neurons in an image region are synchronized in phase. For example, our system for an image with two image regions is simplified as a model with a global inhibitor and two neurons without excitatory coupling; we call it the two-coupled system. Figure 3 plots the bifurcation sets of a fixed point observed in the two- and three-coupled systems. In the analysis, the values of the system parameters (except for k_r and ϕ) were set to $k_f = 0.5$, $d_1 = d_2 = 2$, $W_z = 15$, $\theta_z = 0.5$, $W_x = 15$, $\theta_c = 0$, $\alpha = 4$, $a = 0.5$, $\theta_f = 15$, $\theta_d = 0$, and $\varepsilon = 0.1$. The NS^1_ℓ denotes a Neimark-Sacker bifurcation curve of the fixed point, where the subscript series number ℓ was appended to distinguish between bifurcation sets of the same type. The stable fixed point exists only in the shaded parameter region and is destabilized at the Neimark-Sacker bifurcation points. Multiple Neimark-Sacker bifurcations occur at parameter values on the curve NS^1_1. For example, in the two-coupled system, the number of characteristic multipliers that are outside of the unit circle is changed from 0 to 4 when the value of k_r passes through the curve NS^1_1 from the inside to the outside of the shaded region; in the three-coupled system, its quantity is changed from 0 to 6.

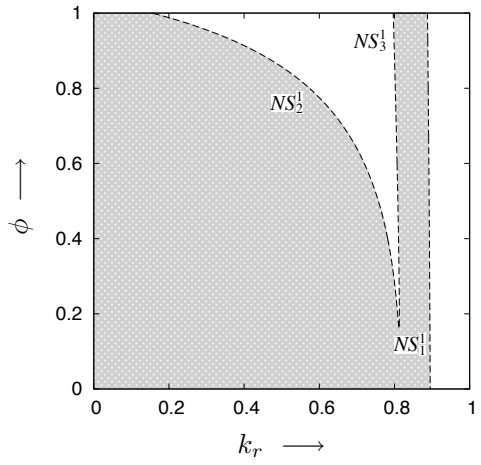

Figure 3: Bifurcation diagram on fixed point observed in reduced model [2, 3].

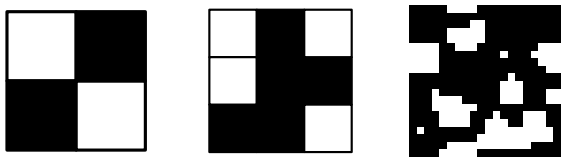

(a) 2×2 pixels (b) 3×3 pixels (c) 20×20 pixels

Figure 4: Black and white images.

4. Experimental Results and Discussion

Let us consider the relevance between the arrangement of characteristic multipliers of a fixed point when it bifurcates and the number of image regions in an input image. To simplify the problem, we treated only binary (black and white) images, shown in Figs. 4(a)–4(c). The dimension numbers in our system to segment 2×2, 3×3, and 20×20 images are 9, 19, and 801, respectively. Here, we set $k_r = 0.88974207$ and $\phi = 0.8$ that correspond to a near point at NS^1_1 in Fig. 3. We also set $d_i = 2$ and $d_j = 0$ in the ith and jth neurons corresponding to white and black pixels, respectively. The values of the other parameters were set to the values described in Sec. 3.

First, in our system for the 2×2 image with two white image regions and two black pixels, we found a fixed point $\boldsymbol{x}^* = (32.096, -31.565, -1.756, 1.516, -1.756, 1.516, 32.096, -31.565, 0.222)^\top$ at the parameter values; its characteristic multipliers were $(0.5, 0.5, -0.8, 0.964 - 0.266i, 0.964 + 0.266i, 0.964 + 0.266i, 0.964 - 0.266i, -2.162, -2.162)^\top$. The numbers of characteristic multipliers inside and outside of a unit circle in the complex plane are three and two, respectively. The four residual ones consist of two pairs of complex conjugates on the circumference of the unit circle (i.e., those that caused the double Neimark-Sacker bifurcations), which makes this consistent with the analyzed results of the two-coupled system [2]. Figure 5(a) plots the characteristic multipliers on the inside, left outside, and circumference of the unit circle as black, red, and blue points, respectively. Note that some points overlap.

Second, we found a fixed point in our system for the 3×3 image with three white image regions and five black pixels, which can be reduced to a three-coupled system. The characteristic multipliers of the fixed point were $(0.5, 0.5, 0.5, 0.5, 0.5, 0.5, 0.694, -0.8, 0.964 - 0.266i, 0.964 + 0.266i, 0.964 - 0.266i, 0.964 + 0.266i, 0.964 - 0.266i, 0.964 + 0.266i, -2.162, -2.162, -2.162, -2.162, -2.162)^\top$ and are plotted in Fig. 5(b). The numbers of characteristic multipliers on the inside, outside, and circumference of the unit circle in the complex plane are 8, 5, and 6, respectively. These three pairs of complex-conjugate characteristic multipliers give rise to triple Neimark-Sacker bifurcations, which is also consistent with the analyzed results of the three-coupled system [3].

The results led us to the following hypotheses.

1. The number of pairs of complex-conjugate characteristic multipliers that cause multiple Neimark-Sacker bifurcations is equal to the number of image regions.

2. The number of characteristic multipliers arranged on $(-\infty, -1)$ is equal to the number of black pixels corresponding to background regions.

3. The other characteristic multipliers are arranged inside of a unit circle.

In other words, if we compute the number of pairs of complex-conjugate characteristic multipliers that cause multiple Neimark-Sacker bifurcations of a fixed point, we can identify the number of image regions to be segmented in a given image.

To test the hypotheses, we computed a fixed point and its characteristic multipliers in our system for the 20×20 image with 10 white image regions and 273 black pixels; the characteristic multipliers are plotted in Fig. 5(c). Results showed that the number of characteristic multipliers arranged on the left outside of the unit circle was 273 and corresponded to the number of black pixels, and the pairs of complex-conjugate characteristic multipliers was 10, which corresponded to the white image regions. This demonstrates that our hypothesis is effective and suggests that our method to identify the number of image regions to be segmented in a given image is also effective.

5. Concluding Remarks

We considered the relevance between the number of image regions to be segmented in a given image and the arrangement of the characteristic multipliers of a fixed point when it bifurcates. Results showed that the number of image regions is the same as the number of characteristic multipliers that multiple Neimark-Sacker bifurcations of a fixed point cause. This demonstrates the suitability of our method to identify the number of image regions. In our future work, we aim to apply our approach to gray-scale images, texture images, and color images using a multi-scaling method [5].

This research is partially supported by the Aihara Innovative Mathematical Modelling Project, the Japan Society for the Promotion of Science (JSPS) through the "Funding Program for World-Leading Innovative R&D on Science and Technology (FIRST Program)," initiated by the Council for Science and Technology Policy (CSTP).

References

[1] K. Fujimoto, M. Musashi, and T. Yoshinaga, "Discrete-time dynamic image segmentation system," *Electron. Lett.*, vol.44, pp.727–729, 2008.

[2] K. Fujimoto, M. Musashi, and T. Yoshinaga, "Reduced Model of discrete-time dynamic image segmentation system and its bifurcation analysis," *Int. J. Imaging Syst. Technol.*, vol.19, pp.283–289, 2009.

[3] M. Kobayashi, K. Fujimoto, and T. Yoshinaga, "Bifurcations of oscillatory responses observed in discrete-time coupled neuronal system for dynamic image segmentation," *J. Signal Processing*, vol.15, pp.145–153, 2011.

[4] H. Kawakami, "Bifurcation of periodic responses in forced dynamic nonlinear circuits: computation of bifurcation values of the system parameters," *IEEE Trans. Circuits Syst.*, vol.31, pp.248–260, 1984.

[5] L. Zhao, R.A. Furukawa, and A.C. Carvalho, "A network of coupled chaotic maps for adaptive multi-scale image segmentation," *Int. J. Neural Syst.*, vol.13, pp.129–137, 2003.

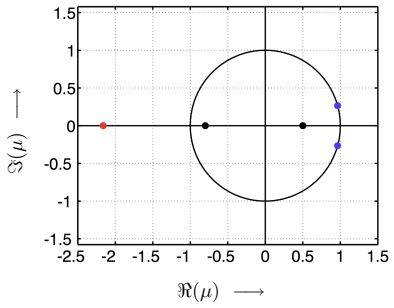

(a)

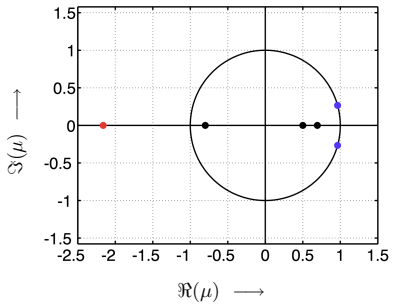

(b)

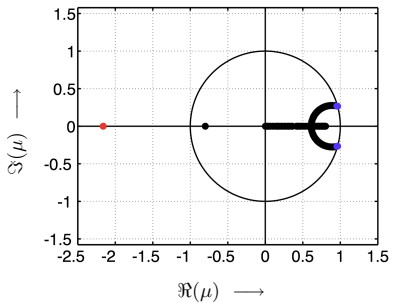

(c)

Figure 5: Arrangement of characteristic multipliers of fixed point in proposed system for (a) 2×2 image, (b) 3×3 image, and (c) 20×20 image. $\Re$ and $\Im$ correspond to the real and imaginary part of the complex number.